



Effects of cryogenic cooling on the spectral luminescence of BACs in bismuth-doped aluminosilicate fiber

MENGYAO ZHANG,¹ , QIANCHENG ZHAO,^{1,*} YUNCONG YANG,¹
CHANGYUAN YU,² , GANG-DING PENG,³ AND TAO ZHU¹

¹Key Laboratory of Optoelectronic Technology and Systems, Education Ministry of China, Chongqing University, Chongqing 400044, China

²Photonics Research Center, Department of Electronic and Information Engineering, The Hong Kong Polytechnic University, Hong Kong SAR, China

³Photonics and Optical Communications Group, School of Electrical Engineering University of New South Wales, Sydney NSW 2052, Australia

*qianchengzhao@cqu.edu.cn

Abstract: The results of liquid nitrogen cooling (LNT, 77 K) on the spectral properties of bismuth-doped aluminosilicate fibers (BDFs) have been presented under varying pump wavelengths. It is revealed that the spectral luminescence of bismuth active centers (BACs) is mildly affected upon excitation at 405, 532, and 980 nm at LNT, whereas notable luminescence enhancement (~ 1.3 times) is observed in the range of 1100–1350 nm (BACs-Al) under 830 nm pumping. The experimental data on the luminescence shape and kinetics of BACs-Al have been obtained at both room temperature (RT) and LNT with varied pumping powers. It is revealed that the enhanced luminescence is caused by the steep rise of emission around 1300 nm (denoted as BAC-Al (II)), which is more efficiently stimulated at a lower temperature. The key laser parameters of BACs have also been evaluated at both RT and LNT. The obtained results may shed some light on the NIR-emitting nature of BACs, and provide a promising strategy for tuning the spectral NIR luminescence scheme of BDFs.

© 2024 Optica Publishing Group under the terms of the [Optica Open Access Publishing Agreement](#)

1. Introduction

Since the first demonstration of near-infrared (NIR) broadband luminescence in the range 1000–1300 nm from bismuth (Bi)-doped aluminosilicate glass in 1999 [1], this novel laser-active medium has attracted enormous attention, intending to develop broadband active components in the optical fiber communication band. To date, a myriad of Bi-doped devices (crystals, glasses, optical fibers) have been created to generate broadband luminescence, gain, and lasing covering the spectral range of 1.1–1.8 μm . The ultra-broadband luminescence of bismuth is proved to benefit from the formation of various bismuth active centers (BACs) coordinated to silicon (BAC-Si), phosphorus (BAC-P), aluminum (BAC-Al), germanium (BAC-Ge), etc [2]. Among these BACs, the luminescence properties and energy levels of BAC-Si and BAC-Ge have been well established, with central luminescent wavelengths at 1430 and 1650 nm, respectively [3,4]. However, the investigations of BAC-Al's spectral properties seem to be challenging since the central luminescence wavelength of BAC-Al is proved to be closely related to the pump wavelength and thus covers a relatively broad wavelength range of 1.1–1.3 μm [3,5]. Moreover, it has turned out that the laser efficiency ($\eta \sim 25\%$) based on the Bi-doped optical fibers with Al_2O_3 - SiO_2 host is the lowest of the family of Bi-doped lasers. Therefore, it is of particular interest to investigate the spectroscopic properties of Bi-doped aluminosilicate fibers within this spectral range. Recently, it has been found that temperature has played a significant role in the formation of BACs. Under an appropriate thermal annealing process, the concentration of

BACs could be increased, which resulted in the enhancement of luminescence intensity and gain coefficients in the range of 1400-1650 nm (BAC-Si and BAC-Ge) [6,7]. Conducting research in this direction, it turns out that the study of cooling effect on the spectral properties of Bi-doped aluminosilicate fibers is very limited, the only research investigates the influence of cooling on the spectral properties of BACs by sweeping the pump wavelengths from 710 to 980 nm. However, the pump power is below 2 mW, which is far below the saturation states of BACs to see the full spectral profiles. Moreover, the spectral luminescence performance pumping at visible range is not presented [8]. Apparently, leading research in the direction of low-temperature zones may provide important information about the nature of BACs. The photoinduced effects (e.g., laser irradiation), or fluorescence dynamics of BACs may also be impacted in the low-temperature zone [9], which may shed some light on the nature of NIR-emitting BACs.

In this regard, herein, the spectral behaviors of BACs, including luminescence properties, have been investigated in Bi-doped aluminosilicate fibers at liquid nitrogen temperature (LNT, 77 K). The temperature-induced changes in the luminescence spectra of BACs have also been studied among various pumping wavelengths, which provides new information on the nature of NIR-emitting BACs.

2. Experimental schemes and results

The Bi-doped aluminosilicate fiber (BDF) under test was manufactured by the conventional modified chemical vapor deposition (MCVD) process. The bismuth and aluminum oxide were deposited in the pure silica tube (Heraeus 300) via the atomic layer deposition (ALD) method with precursors of $\text{Bi}(\text{thd})_3$ and $\text{Al}(\text{CH}_3)_3$, and no phosphorus was introduced during the fabrication process. During the precursor deposition process, the temperature of $\text{Bi}(\text{thd})_3$ was controlled in the range 150-250°C. The key dopants, including Bi and Al ions, were estimated to be 150-180 and 350-750 ppm in the fiber preform (preform slice, ~1 mm thickness) via Electron Probe Micro-Analyzer (EPMA) measurement. Subsequently, GeO_2 is doped by MCVD method forming the improved higher index core layer, and collapsed into solid and transparent Bi-doped preform. The doped silica preform was drawn into an optical fiber with a core and cladding diameter of 9.6 and 124 μm , and the refractive index of the drawn fiber was measured to be around 6.0×10^{-3} by optical fiber analyzer (see Fig. 1(a)). Firstly, the small-signal absorption spectrum of our homemade BDF was measured with a conventional cut-back method using the monochromator-lockin amplifier system. The measured small-signal absorption spectrum of BDF across the visible and NIR regions is shown in Fig. 1(b).

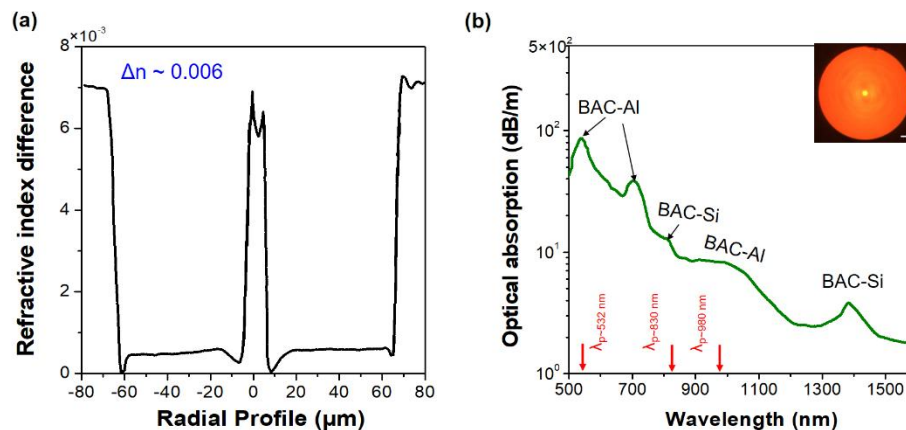


Fig. 1. (a) Refractive index profile of drawn BDF. (b) Optical absorption spectrum of BDF in the range of 500-1700nm; Scale bar = 20 μm .

As can be seen from Fig. 1(b), there exist two groups of absorption bands that are related to BACs, namely, BAC-Al absorption bands at 500, 700, and 1000 nm, and BAC-Si absorption bands at 816 and 1400 nm (which are partially overlapped with [10,11]). To understand the cooling effect on the spectroscopic properties of BACs in our homemade BDF, the backward luminescence of BDF is investigated with several pumping wavelengths at both room temperature (RT, 300 K) and LNT. The measurement scheme of backward luminescence of BDF is shown in Fig. 2. A short piece of BDF ($L \sim 2$ cm, to prevent nonlinear effects such as reabsorption, excited state absorption) was fully immersed in the Dewar (~ 1 Liter) to maintain the cryogenic temperature. The spectral luminescence of BDF was recorded backward with an optical spectral analyzer (OSA, Agilent 86140B) via the broadband wavelength division multiplexer (WDM). The pump source was varied with multiple wavelengths to investigate the changes in luminescence bands at both RT and LNT.

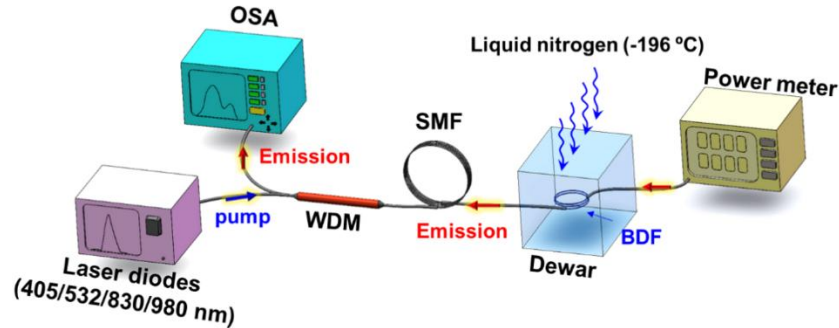


Fig. 2. Schematic of backward luminescence under various pump wavelengths at both RT and LNT.

Firstly, the results of luminescence spectra of BDF under visible wavelength laser pumping (405 and 532 nm) are presented in Figs. 3(a) and 3(b) at both RT and LNT.

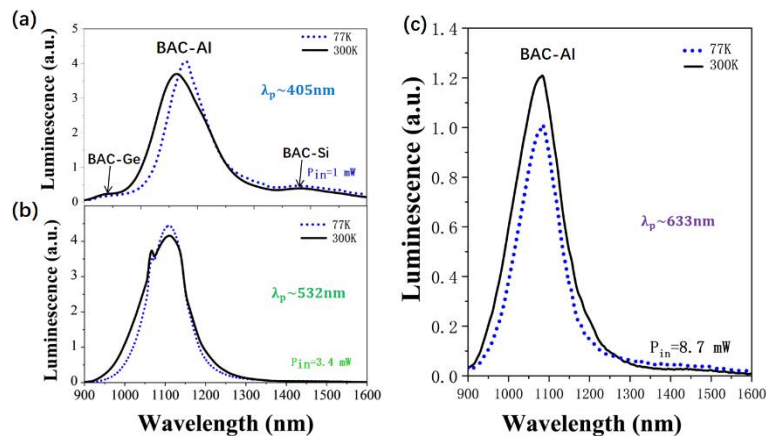


Fig. 3. Luminescence spectra of BACs at both RT and LNT under (a) 405 nm pumping, (b) 532 nm pumping, and (c) 633 nm pumping.

Obviously, under all pumping wavelengths, there exists a dominant luminescence band centering around 1100 nm, which is ascribed to BAC-Al [3]. However, it is seen that more luminescence bands are excited under 405 nm pumping, which belongs to BAC-Ge (~ 950 nm) and BAC-Si (~ 1430 nm), whereas only one predominant luminescence peak of BAC-Al is observed

under 532 nm pumping and 633 nm pumping. Under the cooling effect of liquid nitrogen temperature, the shape of the luminescence spectrum did not change significantly. It is worth noting, however, the full width at half maximum (FWHM) bandwidth narrowing of the dominant peak of BAC-Al is observed (~ 20 nm) at all pump wavelengths. The bandwidth narrowing is mainly attributed to the suppression and weakening effect of homogeneous broadening at a relatively low temperature [12]. In addition, the integrated luminescence intensity as a function of input pump power ($\lambda_p \sim 532$ nm) at both RT and LNT is also measured and presented in Fig. 4.

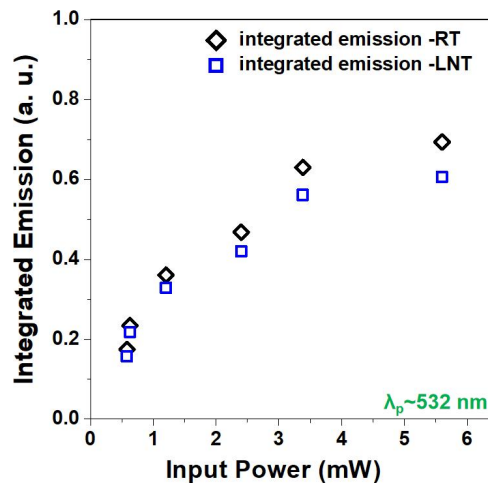


Fig. 4. Integrated luminescence spectra of BACs with varying pump powers at 532 nm at both LNT and RT.

As can be seen from Fig. 4, the integrated luminescence intensity of BAC-Al increases steadily with increasing pump power at both temperatures and approaches saturation when the pump power is beyond 5 mW. Moreover, it is expected that within experimental error, the spectral luminescence behavior at 77 K is the same as at 300 K, indicating that the quantum efficiency doesn't truly change with changing temperature in such a big range. This suggests the stable and favorable spectral performance of BDFs for practical spectroscopic applications related to temperature. In addition, the luminescence spectra under CW NIR laser pumping at both LNT and RT are also measured. Firstly, the luminescence results of BDF at both temperatures under 980 nm pumping are presented, as shown in Fig. 5.

Similar to the previous short pump wavelengths studied, the cryogenic temperature at 77 K doesn't have much influence on the spectral shape of BAC-Al, only with the narrowing of bandwidth from 126 to 106 nm. When the pump power rises to 80 mW, the luminescence curves at 980 nm are obviously dense at both RT and LNT, indicating that this state is approaching saturation. The quantum efficiency doesn't change with the cooling effect, which is proved by the constant integrated luminescence intensity ratio of ~ 1.03 between LNT and RT. Finally, the cooling effect on the spectral luminescence of BACs is studied under CW 830 nm laser pumping, and the results are shown in Figs. 6(a) and 6(b). Vastly different from other pumping wavelengths described previously, under 830 nm pumping, significant change in the shape of luminescence spectra of BACs is observed, with notable increase and broadening of luminescence bands in the range 1000-1350 nm (See inset of Fig. 6(a)), whereas the luminescent band of BAC-Si remains unchanged at LNT cooling (only the FWHM has been decreased from 105 to 82 nm). At both RT and LNT, the luminescence intensity of BACs increases steadily with increasing pump powers, and no saturation is shown at the maximum pump power of ~ 100 mW. Moreover, compared to other pump wavelengths described above, pumping at 830 nm enables the optical transition

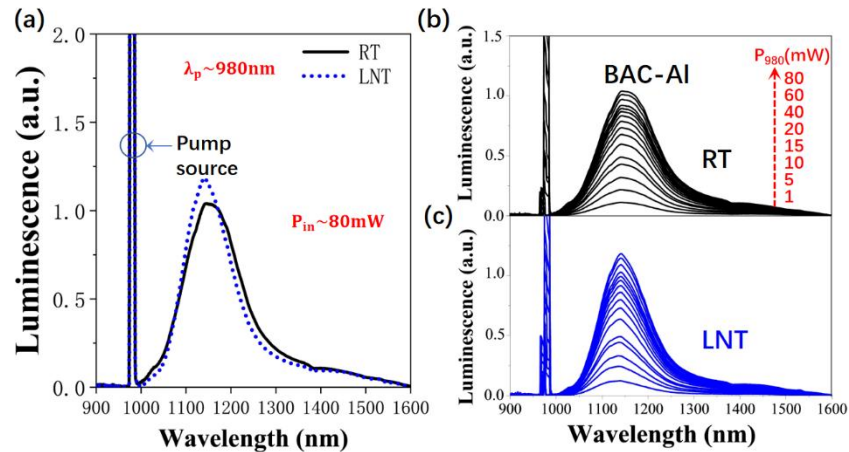


Fig. 5. (a) Luminescence spectra of BACs at both RT and LNT under 980 nm pumping with 80 mW. Luminescence spectra of BACs under 980 nm pumping with varying pump power at (b) RT and (c) LNT.

of multiple BACs which contribute to broadband spectral luminescence, and thus is preferred wherever NIR broadband luminescence or amplification is required.

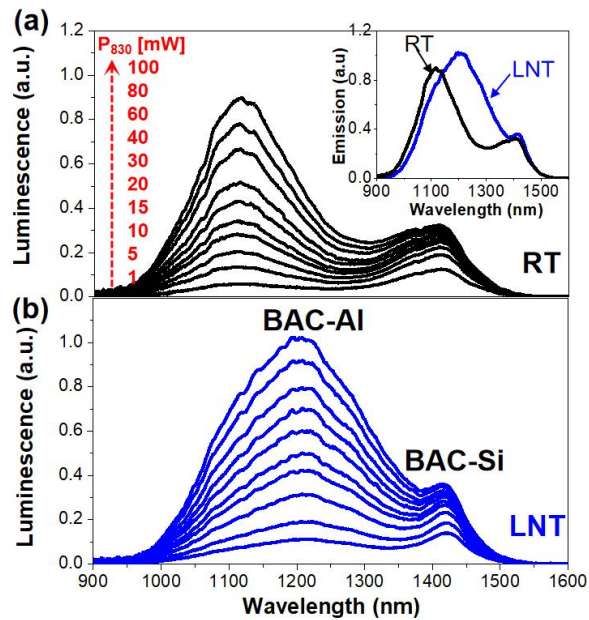


Fig. 6. Luminescence spectra of BACs under 830 nm pumping with varying pump power at (a) RT and (b) LNT. Inset: luminescence spectra comparison between RT and LNT at 830 nm excitation ($P_{in} \sim 100$ mW).

To elucidate more clearly the spectral change, precise Gaussian decomposition, as an effective way to analyze complex host glass matrix [13–15], was applied to the complex luminescence spectra ($R^2 \sim 0.9998$). The decomposed results are depicted in Figs. 7(a) and 7(b).

Clearly, in addition to the well-known luminescence bands centering around 1100 nm (defined as BAC-Al (I)) and BAC-Si at 1430 nm, there features another luminescent band peaking around

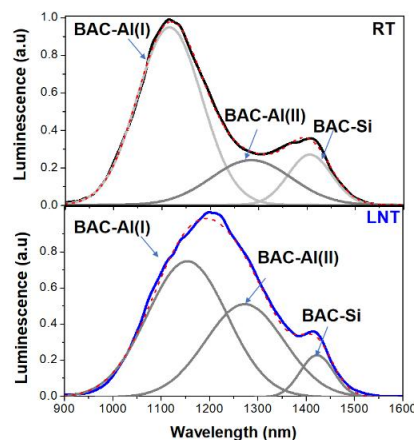


Fig. 7. Gaussian decomposition of spectral luminescence of BACs under 830 nm pumping at (a) RT and (b) LNT.

1300 nm, which is labeled as BAC-Al (II). The reason why this luminescence band is ascribed to the BACs coordinated to aluminum is that no luminescence band is observed in this spectral range with pure Bi-doped silica-based fibers [4]. To further elaborate on this peculiarity, time-resolved fluorescence spectroscopy has been applied to study the kinetics of Bi-related luminescence bands under 830 nm pumping ($P_{in} \sim 100$ mW), the detailed measurement setup and principle are similar to that described in [16]. The luminescence decay curves in the logarithm scale at typical wavelengths at LNT are presented in Fig. 8(a). As seen from Fig. 8(a), the straight decay curves prove that they follow the single exponential decay trend and are distinguished with 716 μ s at 1100 nm and 452 μ s at 1300 nm, this strongly suggests the independence of each Bi-related emitting band. Moreover, the two sub-bands of BAC-Al are clearly distinguished and grouped, evidenced by notable lifetime differences between two groups of peak wavelengths (see inset of Fig. 8(a)). Similar phenomenon is observed at RT, with two groups of luminescence lifetimes at or around distinct peak wavelengths. It should be noted that the luminescence lifetime of BAC-Al (~ 20 -30 μ s) is slightly reduced at RT due to the intensified phonon-assisted non-radiative transition as compared to that of LNT. While the inherent physicochemical structure of BAC-Al (II) remains ambiguous. It can be referred that this luminescence band should belong to the same generic of BAC-Al but with different microstructures compared to that of BAC-Al (I).

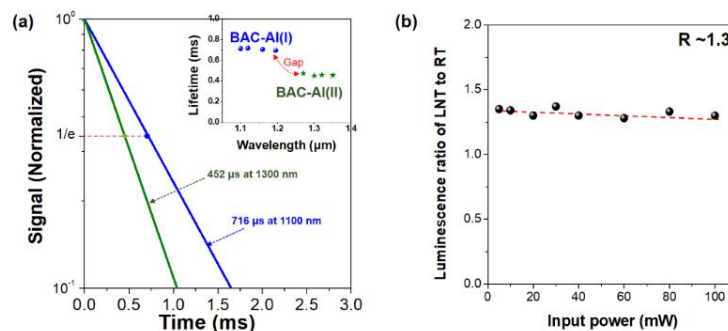


Fig. 8. (a) Luminescence decay of BACs at featured emission wavelengths. (b) Luminescence intensity ratio of LNT to RT with varying pump power at 830 nm.

Obviously, by cryogenic cooling of our homemade BDFs, the emission of BAC-Al (II) is facilitated noticeably and becomes dominant over all the emission bands, which in turn bridges the luminescence between BAC-Al (I) and BAC-Si. Thus, broadband and enhanced luminescence intensity are observed at LNT under 830 nm pumping. Benefiting from the steep rise of luminescence intensity of BAC-Al (II) around 1300 nm, the quantum efficiency has been improved by 1.3 times with all available pump powers, when the fiber is working in the liquid nitrogen temperature, as plotted in Fig. 8(b). It should be noted that the luminescence spectra of BACs recover to the original shape once the fiber is pulled out of the liquid nitrogen environment and tested at RT. This differs from the phenomenon reported in [17]. Thermal quenching of the fibers in [17] similarly leads to an enhancement of the luminescence intensity of BAC-Al(II) in BACs, but this effect is irreversible. Apparently, the rearrangement of the glass matrix in Bi-doped fibers by cryogenics is temporary and essentially does not affect the luminescent structure of the BACs themselves. This is different from the effect of thermal quenching on the fiber.

Currently, there are findings suggesting that oxygen-deficient centers (ODCs) play an important role in the formation of BACs [18]. The presence of this defect in the local environment of Bi ion leads to the appearance of optical transitions in the near-infrared range. We speculate that the significant changes in the spectral properties of bismuth-doped fibers observed during thermal treatment are related to the modification of the glass network around the bismuth ions. These processes are triggered by the influence of the ODC, which acts as a sensitive structural unit of the glass host and may lead to the disruption/formation of the BACs [7]. We consider that cryogenic cooling did not induce fundamental changes in ODCs. To prove this, more experiments on the underlying mechanisms of BACs are needed for further verification.

However, it has revealed that there does exist a novel luminescence band that is very sensitive to environmental temperature. To further evaluate our homemade BDF as a potential gain medium, the stimulated emission cross sections σ_e at typical emission wavelengths of BAC-Al are calculated according to the Füchtbauer–Landenburg equation [19,20]:

$$\sigma_e = \frac{\lambda^2 * g(v)}{8\pi n^2 \tau} \quad (1)$$

Where λ is the wavelength, τ is the fluorescence lifetime, n is the refractive index of the host material ($n = 1.48$ in our case), and $g(v)$ is the line shape function for emission in frequency domain. Assuming a Gaussian-shaped band is applied to the emission of BACs designated for complex host matrix and multiple emitting centers, Eq. (1) can be rewritten as [21]:

$$\sigma_e = \frac{\lambda_0^2}{4\pi n^2 \tau \Delta V} \left(\frac{\ln 2}{\pi} \right)^{1/2} \quad (2)$$

Where λ_0 is the central wavelength of the emission band, ΔV is the FWHM of the emission in the frequency domain ($\Delta v = \Delta \lambda * c / \lambda^2$). Applying all the available information into Eq. (2). The emission cross sections of BAC-Al(I) and BAC-Al (II) at LNT are estimated as: 7.9×10^{-21} and 1.7×10^{-20} cm², with about a 15% increase of σ_e as compared to those at RT. These calculated values of σ_e are comparable and of the same order of magnitude (10^{-20} cm²) to other Bi-doped aluminosilicate glasses [22,23], proving the reliability of our obtained parameters and calculations. More specifically, it is anticipated that a higher gain should be achieved at a lower temperature due to the relatively large σ_e at LNT. In addition, the product of σ_e and τ for BACs-Al has also been estimated because it is an important parameter to characterize laser materials where the laser threshold is proportional to $(\sigma_e \times \tau)^{-1}$, the product $\sigma_e \tau$ of BAC-Al(I) and BAC-Al(II) at LNT are calculated as: 5.68×10^{-24} cm²s and 7.75×10^{-24} cm²s, respectively. The products of $\sigma_e \times \tau$ for BACs-Al in the range 1100-1300 nm are bigger than Ti: Al₂O₃ (3.1×10^{-24} cm²s) and Ni²⁺-doped ZnO–Al₂O₃–SiO₂ glass (3.1×10^{-24} cm²s) [15], and comparable to Erbium-doped

silicate fiber or glass ($\sim 4.1 \times 10^{-23} \text{ cm}^2\text{s}$). Despite the fact that the long metastable lifetime (8–10 ms) from $^4\text{I}_{13/2}$ of Er^{3+} favors the laser transitions for EDFs, it is noticeable that Bi-doped aluminosilicate fibers, especially operating at low temperatures, could also be a promising host for broadband amplifiers since the product of σ_e and FWHM of BACs-Al are relatively high ($\sim 329 \times 10^{-20} \text{ cm}^2\cdot\text{nm}$ for BAC-Al (II) at LNT).

In Er-doped silica-based fibers, the crystalline field of the host materials causes Stark splitting of Er^{3+} energy levels, and further inhomogeneous broadening is usually caused by differences of Er ion sites located in amorphous host glass [24–26]. In the case of Bi-doped silica-based multicomponent fibers, it is undoubted that the diversity and complexity of Bi ion sites contribute to the creation of multiple NIR-emitting BACs as well as the linewidth broadening for each emission band. In the LNT environment, the homogeneous broadening effect is restricted due to the reduced nonradiative transition rates for solid medium [27]. Therefore, the emission linewidth should be narrowed in the cryogenic temperature for Bi-related emission bands, which has been verified in other types of BACs (e.g., BAC-Si, BAC-Ge). The peculiarity of linewidth broadening for BAC-Al at LNT suggests that it should be comprised of at least two luminescence bands. Indeed, similar broadening phenomenon for Bi-doped aluminosilicate fibers ($96.7\text{SiO}_2:3.3\text{Al}_2\text{O}_3$) is also reported in [28], where a distinct luminescent band peaking at 1300 nm was observed upon 860 nm pumping at LNT. However, neither the pump wavelength dependence nor detailed lifetime analysis was performed. In another sense, although the 3D contour plot was conducted in [3] with pump wavelength sweeping of Bi-doped aluminosilicate fiber at LNT, still, the pump power dependence, luminescence kinetics, and the detailed spectral analysis were not conducted there. Moreover, one can see that the emission intensity distribution shifts towards a longer wavelength at LNT from Ref. [3]. These experimental results and the previous studies all suggest that the second luminescence band of BAC-Al is more active at a lower temperature upon short wavelength pumping. Besides, it is also found that the secondary luminescence peak of BAC-Al (designated as “NIR-II”, $\lambda_p \sim 1250 \text{ nm}$, FWHM $\sim 310 \text{ nm}$) is closely related to the doping level of Bi in bulky Bi-doped aluminosilicate glass [29], and the origin of this band is presumably attributed to $\text{Bi}^+ - \text{Bi}^+$ dimers. Up till now, the exact physical model of NIR Bi-related centers remains debatable (e.g., Bi^+ , Bi^0 , Bi-O molecule, Bi_2 [2,30]). However, it has been repeatedly reported that Bi^+ ion (so-called “Bi in the low valent state”, $[\text{AlO}_4/2]^-$, Bi^+) should be most likely responsible for the NIR luminescence in aluminosilicate glass networks [31]. Still, the NIR emitting nature of BAC-Al (II) in our homemade BDF remains ambiguous, further spectroscopic research, including time-resolved spectroscopy, and Raman spectral analysis, may be required to investigate deeper into the novel band emitting around 1300 nm.

Fortunately, the broadband characteristics of BAC-Al, together with other types of BACs and Er^{3+} , spread over the entire fiber-optic communication band from 1100 to 1600 nm. The featured luminescence bands for different BACs and Er^{3+} are illustrated in Fig. 9(a). It is seen that the operating wavelength bands of BAC-Al, BAC-P, and BAC-Si are located adjacently to each other, it is anticipated that multiple BACs could be stimulated at only one pump wavelength. Therefore, Bi-doped silica-based fibers with multiple dopants and optimized doping levels are favored, especially on occasions when broadband optical amplification is needed. Moreover, the possible low-lying energy levels of BACs-Al have also been constructed upon 830 nm pumping, as shown in Fig. 9(b). At RT, the optical transition of BAC-Al(I) takes dominance and gives rise to emission around 1100 nm. Under liquid nitrogen cooling, the emission of BAC-Al(II) becomes predominant at the expense of BAC-Al(I), which may be caused by energy redistribution between BACs or inter-band energy transfer from BAC-Al(I). Apparently, pumping around 830 nm with a low temperature facilitates the optical transition of BAC-Al(II) at 1300 nm, and hence results in higher luminescence efficiency and greater bandwidth over the NIR spectral range.

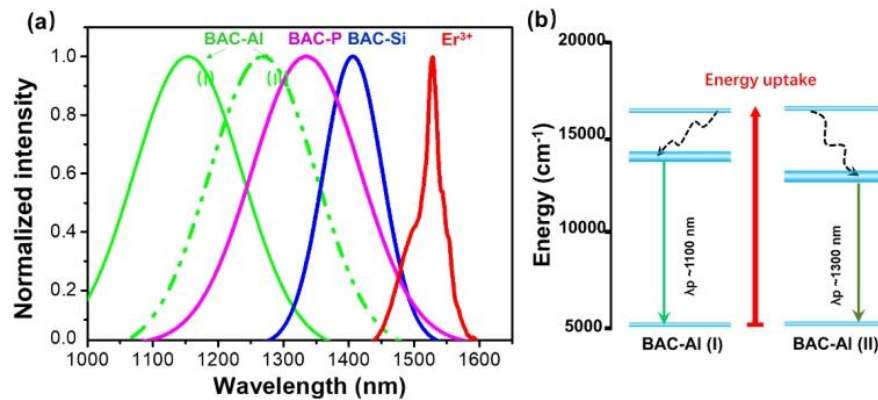


Fig. 9. (a) Characteristic luminescence bands of main BACs and Er^{3+} . (b) Low-lying energy levels for BAC-Al(I) and BAC-Al (II) under 830 nm pumping.

3. Conclusions

In conclusion, the spectral luminescence performance of our homemade Bi-doped aluminosilicate fibers has been investigated at both RT and LNT with different pumping wavelengths. It is found that cooling under LNT results in no significant change to the spectral luminescence of BACs for most of the pumping wavelengths, whereas pumping at 830 nm by cryogenics greatly facilitates the NIR luminescence intensity and bandwidth of BACs-Al. The mechanism of enhanced luminescence performance at LNT of BACs-Al is also analyzed by time-resolved fluorescence spectroscopy, which is found to be linked with the sharp rise of BAC-Al (II) located at 1300 nm. Furthermore, the key parameters ($\sigma_e \times \tau$) of BACs have also been estimated towards evaluating our homemade BDFs as a practical gain medium, along with the construction of low-lying energy levels of BACs-Al. These spectroscopic results may shed some light on the NIR emitting center of BAC-Al, and provide useful information for Bi-doped aluminosilicate fibers operating in the O-band for fiber-optic-based communication and sensing.

Funding. Fundamental Research Funds for the Central Universities (2024CDJXY008); National Natural Science Foundation of China (61520106014, 61675032); Chongqing University Research Start-up Funding (02100011080003).

Acknowledgment. Authors are thankful for the fruitful suggestions and experimental advice from Prof. Changyuan Yu from the Hong Kong Polytechnic University.

Disclosures. The authors declare no conflicts of interest.

Data Availability. Data underlying the results presented in this paper are not publicly available at this time but may be obtained from the authors upon reasonable request.

References

1. K. Murata, Y. Fujimoto, T. Kanabe, *et al.*, "Bi-doped SiO_2 as a new laser material for an intense laser," *Fusion Eng. Des.* **44**(1-4), 437–439 (1999).
2. E. M. Dianov, "Nature of Bi-related near IR active centers in glasses: state of the art and first reliable results," *Laser Phys. Lett.* **12**(9), 095106 (2015).
3. S. V. Firstov, V. F. Khopin, I. A. Bufetov, *et al.*, "Combined excitation-emission spectroscopy of bismuth active centers in optical fibers," *Opt. Express* **19**(20), 19551–19561 (2011).
4. I. A. Bufetov, S. L. Semenov, V. V. Vel'miskin, *et al.*, "Optical properties of active bismuth centres in silica fibers containing no other dopants," *Quantum Electron.* **40**(7), 639–641 (2010).
5. L. I. Bulatov, V. M. Mashinskii, V. V. Dvoirin, *et al.*, "Luminescent properties of bismuth centres in aluminosilicate optical fibers," *Quantum Electron.* **40**(2), 153–159 (2010).
6. S. Wei, Y. Luo, D. Fan, *et al.*, "BAC activation by thermal quenching in bismuth/erbium codoped fiber," *Opt. Lett.* **44**(7), 1872–1875 (2019).
7. S. V. Firstov, S. V. Alyshev, V. F. Khopin, *et al.*, "Effect of heat treatment parameters on the optical properties of bismuth-doped $\text{GeO}_2\text{:SiO}_2$ glass fibers," *Opt. Mater. Express* **9**(5), 2165–2174 (2019).

8. Q. Zhao, Y. Luo, Y. Dai, *et al.*, "Effect of pump wavelength and temperature on the spectral performance of BAC-Al in bismuth-doped aluminosilicate fibers," *Opt. Lett.* **44**(3), 634–637 (2019).
9. Q. Zhao, Y. Luo, Y. Tian, *et al.*, "Pump wavelength dependence and thermal effect of photobleaching of BAC-Al in bismuth/erbium codoped aluminosilicate fibers," *Opt. Lett.* **43**(19), 4739–4742 (2018).
10. V. V. Dvoyrin, A. V. Kir'yanov, V. M. Mashinsky, *et al.*, "Absorption, gain, and laser action in bismuth-doped aluminosilicate optical fibers," *IEEE J. Quantum Electron.* **46**(2), 182–190 (2010).
11. I. Razdobreev, H. E. Hamzaoui, V. Y. Ivanov, *et al.*, "Optical spectroscopy of bismuth-doped pure silica fiber preform," *Opt. Lett.* **35**(9), 1341–1343 (2010).
12. C. A. Millar, T. J. Whitley, and S. C. Fleming, "Thermal properties of an erbium-doped fiber amplifier," *IEEE Proc.-J: Optoelectron.* **137**(3), 155–162 (1990).
13. M. Peng, J. Qiu, D. Chen, *et al.*, "Superbroadband 1310 nm emission from bismuth and tantalum codoped germanium oxide glasses," *Opt. Lett.* **30**(18), 2433–2435 (2005).
14. S. Wei, Y. Luo, M. Ding, *et al.*, "Thermal effect on attenuation and luminescence of Bi/Er Co-doped fiber," *IEEE Photonics Technol. Lett.* **29**(1), 43–46 (2017).
15. Z. Qiancheng, Y. Luo, and G.-D. Peng, "Broadband Near Infrared (NIR) luminescence spectra of Bi/Er co-doped silicate fiber (BEDF) under 830 and 980 nm dual pumping," in *Optical Fiber Communication Conference (OSA)*, San Diego, USA, Th4A. 7, (2017).
16. A. Zareanborji, H. Yang, G. E. Town, *et al.*, "Simple and accurate fluorescence lifetime measurement scheme using traditional time-domain spectroscopy and modern digital signal processing," *J. Lightwave Technol.* **34**(21), 5033–5043 (2016).
17. Q. Zhao, Y. Luo, Q. Hao, *et al.*, "Effect of thermal treatment parameters on the spectral characteristics of BAC-Al in bismuth/erbium-codoped aluminosilicate fibers," *Opt. Lett.* **44**(18), 4594–4597 (2019).
18. S. Firstov, S. Alyshev, V. Khopin, *et al.*, "Photobleaching effect in bismuth-doped germanosilicate fibers," *Opt. Express* **23**(15), 19226–19233 (2015).
19. W. L. Barnes, R. I. Laming, E. J. Tarbox, *et al.*, "Absorption and emission cross section of Er^{3+} doped silica fibers," *IEEE J. Quantum Electron.* **27**(4), 1004–1010 (1991).
20. Y. Wang, S. Wang, A. Halder, *et al.*, "Bi-doped optical fibers and fiber amplifiers," *Opt. Mater.: X* **17**, 100219 (2023).
21. X. Meng, J. Qiu, M. Peng, *et al.*, "Near-infrared broadband emission of bismuth-doped aluminophosphate glass," *Opt. Express* **13**(5), 1628 (2005).
22. Y. Luo, J. Wen, J. Zhang, *et al.*, "Bismuth and erbium codoped optical fiber with ultrabroadband luminescence across O-, E-, S-, C-, and L-bands," *Opt. Lett.* **37**(16), 3447–3449 (2012).
23. Y. Kuwada, Y. Fujimoto, and M. Nakatsuka, "Ultrawideband light emission from bismuth and erbium doped silica," *Japan. J. Appl. Phys.* **46**(4R), 1531–1532 (2007).
24. C. R. Giles and E. Desurvire, "Modeling erbium-doped fiber amplifiers," *J. Lightwave Technol.* **9**(2), 271–283 (1991).
25. A. Egatz-Gómez, O. G. Calderón, S. Melle, *et al.*, "Homogeneous broadening effect on temperature dependence of green upconversion luminescence in erbium-doped fibers," *J. Lumin.* **139**, 52–59 (2013).
26. E. Desurvire and J. R. Simpson, "Amplification of spontaneous emission in erbium-doped single-mode fibers," *J. Lightwave Technol.* **7**(5), 835–845 (1989).
27. P. M. Becker, A. A. Olsson, and J. R. Simpson, *Erbium-doped Fiber Amplifiers: Fundamentals and Technology* (Elsevier, 1999).
28. V. V. Dvoyrin, V. M. Mashinsky, L. I. Bulatov, *et al.*, "Bismuth-doped-glass optical fibers - a new active medium for lasers and amplifiers," *Opt. Lett.* **31**(20), 2966–2968 (2006).
29. A. Veber, M. R. Cicconi, A. Puri, *et al.*, "Optical properties and bismuth redox in bi-doped high-silica Al-Si glasses," *J. Phys. Chem. C* **122**(34), 19777–19792 (2018).
30. M. Peng, C. Zollfrank, and L. Wondraczek, "Origin of broad NIR photoluminescence in bismuthate glass and Bi-doped glasses at room temperature," *J. Phys.: Condens. Matter* **21**(28), 285106 (2009).
31. V. Dvoyrin, V. Mashinsky, E. Dianov, *et al.*, "Absorption, fluorescence and optical amplification in MCVD bismuth-doped silica glass optical fibers," in *31st European Conference on Optical Communication, ECOC 2005 4*, 949–950 (2005).